BILINGUAL PUBLISHING CO.
Pioneer of Global Academics Since 1984

Semiconductor Science and Information Devices
https://ojs.bilpublishing.com/index.php/ssid

ARTICLE

Intrinsic Photoconductivity of Few-layered ZrS2 Phototransistors via Multiterminal Measurements

Rukshan M. Tanthirige[1] Carlos Garcia[2] Saikat Ghosh[3] Frederick Jackson II[1] Jawnaye Nash[1] Daniel Rosenmann[4] Ralu Divan[4] Liliana Stan[4] Anirudha V. Sumant[4] Stephen A. McGill[2] Paresh C. Ray[1] Nihar R. Pradhan[1,2*]

1. Layered Materials and Device Physics Laboratory, Department of Chemistry, Physics and Atmospheric Science, Jackson State University, Jackson, MS 39217, USA
2. National High Magnetic Field Laboratory, Tallahassee, FL 32310, USA
3. Kunming University of Science and Technology, Kunming 650500, China
4. Center for Nanoscale Materials, Argonne National Laboratory, 9700 S-Cass Avenue, Lemont, IL-60439, USA

ARTICLE INFO

Article history
Received: 4 December 2019
Accepted: 17 December 2019
Published Online: 31 December 2019

Keywords:
Field-effect transistors
Zirconium sulphide
Phototransistor
Responsivity
Quantum efficiency

ABSTRACT

We report intrinsic photoconductivity studies on one of the least examined layered compounds, ZrS_2.Few-atomic layer ZrS_2 field-effect transistors were fabricated on the Si/SiO_2 substrate and photoconductivity measurements were performed using both two- and four-terminal configurations under the illumination of 532 nm laser source. We measured photocurrent as a function of the incident optical power at several source-drain (bias) voltages. We observe a significantly large photoconductivity when measured in the multiterminal (four-terminal) configuration compared to that in the two-terminal configuration. For an incident optical power of 90 nW, the estimated photosensitivity and the external quantum efficiency (EQE) measured in two-terminal configuration are 0.5 A/W and 120%, respectively, under a bias voltage of 650 mV. Under the same conditions, the four-terminal measurements result in much higher values for both the photoresponsivity (R) and EQE to 6 A/W and 1400%, respectively. This significant improvement in photoresponsivity and EQE in the four-terminal configuration may have been influenced by the reduction of contact resistance at the metal-semiconductor interface, which greatly impacts the carrier mobility of low conducting materials. This suggests that photoconductivity measurements performed through the two-terminal configuration in previous studies on ZrS_2 and other 2D materials have severely underestimated the true intrinsic properties of transition metal dichalcogenides and their remarkable potential for optoelectronic applications.

**Corresponding Author:*
Nihar R. Pradhan,
Layered Materials and Device Physics Laboratory, Department of Chemistry, Physics and Atmospheric Science, Jackson State University, Jackson, MS 39217, USA; National High Magnetic Field Laboratory, Tallahassee, FL 32310, USA;
Email: nihar.r.pradhan@jsums.edu

 DOI: https://doi.org/10.30564/ssid.v1i2.1526

1. Introduction

Transition Metal Dichalcogenides (TMDs) is one of the groups of two-dimensional layered crystals coupled through Van der Waals interactions that have attracted great attention in the research community for their promising potential in high performing electronic and optoelectronic devices [1–10]. They inherit strong interaction with light as most of their bandgaps lie in the visible region, high room temperature mobilities and conductivities have given them a unique position in the semiconductor industry [11,12]. Among the layered compounds, including those of group VIB and VIIB elements such as Mo, W and Re have been extensively studied compared to TMDs of group IVB elements; Zr, Hf and Rf. Despite the lack of attention, theoretical investigations suggest those monolayers Zr or Hf based TMDs may exhibit higher mobilities than that of group VIB counterparts [13]. In addition, ZrX_2 compounds (X: chalcogen) predicted to show strain-induced indirect-to-direct bandgap transitions [14,15] and even semiconductor-to-metal phase transitions [16]. MoS_2 has been the most widely studied TMD for its electrical and optical properties, particularly due to its direct bandgap of 1.8 eV in monolayer, tunable layer dependent band structure and natural availability [17,18]. In the monolayer, MoS_2 based field effect transistors (FETs) can achieve high ON/OFF current ratios in the order of 10^8 and high responsivity [19,20]. Previous studies report a wide range of responsivities from mA/W to 10^4 A/W [20–24] for monolayer and few-layered MoS_2 FETs, which depend on the incident optical power, source-drain (bias), back-gate voltages, and the type and quality of electrical contacts. Lopez-Sanchez et al. [20] reported a high responsivity of 880 A/W under a source-drain bias voltage of 8 V and an applied gate voltage of 60 V. However, Choi et al. [25] demonstrated that FETs based on multilayer MoS_2 have wider spectral range, high responsivity and high room temperature mobilities compared to that of monolayer MoS_2 FETs. Tsai et al. [26] observed that few-layered MoS_2 FETs exhibit high broadband gains (13.3), high detectivities (10^{10} $cmHz^{1/2}/W$) and ultrafast photoresponse (rise time of 70 μs and fall time of 110 μs). Pak et. al. [23] reported high responsivities for monolayer MoS_2 when the FET is in the ON state ($V_g > 0$ V), however in contrast, Lee et. al. [27] observed high responsivities for few-layered MoS_2 FETs while in the OFF state ($V_g < 0$ V).

Similar to MoS_2, other TMDs such $MoSe_2$ and WSe_2 have exhibited promising optoelectronic characteristics in both monolayer and few-layered forms [6,8]. Abderrahmane et. al. [28] observed an ultrahigh photosensitivity of 97.1 A/W and an impressive external quantum efficiency (EQE) of 22666% for a few-layered $MoSe_2$ FET at zero gate voltage. These observations signify that optoelectronic properties and transport mechanisms of MoS_2 and other TMD based FETs show a clear difference between monolayer and multilayer forms. WSe_2 is another layered TMD with bandgaps ranging from 1.3 eV (bulk) to 1.8 eV (monolayer) that shows p-type conductivity unlike MoS_2 or $MoSe_2$ [29]. Early studies showed that WSe_2 has a poor responsivity of 8 mW/A when the FET is in the OFF state, which increases drastically when the FET is set to the ON state, but it inherited poor switching speeds of 5 s [30]. In contrast, our previous study on tri-layer WSe_2 crystals synthesized via chemical vapor transport (CVT) showed high speed switching behavior of 5 μs [6]. Our most recent study on few-layered WSe_2 FETs showed promising optoelectronic properties with high responsivity of 85 A/W and ultrahigh EQE of over 19600% [31]. In addition, the metal contact semiconductor interface and the type of metal contacts play an important role on transport properties as they change the height of the Schottky barrier [30]. In addition to the electrical transport, their phototransport properties can be greatly affected by contact resistance [10,31].

Electrical transport measurements of most TMDs were conducted using two metal contacts, where both current and voltage are sourced and measured using the same terminals, in which contact resistance can dominate the transport properties. Although the contacts-driven carrier mobility can be utilized in certain applications such as in gas sensing devices [32], it hinders the ability to investigate intrinsic properties of semiconductor devices. Some of the recent reports claim observing intrinsically higher carrier mobilities and conductivities with four terminal measurements, i.e. two terminals to measure/inject the current and the other two terminals use to sense the voltage drop across the channel [4,9,10,33]. The advantage of four-terminal configuration is that it eliminates the influence of the contact resistance, which is vital when measuring intrinsic material transport properties of materials with low carrier mobilities. For the search of new materials and their functional properties, here we explored the phototransport properties of a few- layered ZrS_2 phototransistor with four terminals, which has not been reported in the literature. The bandgap of bulk ZrS_2 is 1.4 eV,

DOI: https://doi.org/10.30564/ssid.v1i2.1526

whereas the monolayer shows 2 eV [34,35]. The reported mobility of few-layered ZrS_2 FET varies between 0.1 - 1 cm^2/Vs [36–38]. Further, electrical transport studies of the ZrS_2 nanobelts show extremely high photoresponsivity [16] under UV light illumination despite its poor mobility of 1 10^{-5} cm^2/Vs. In this study, we performed photoconductivity measurements of two-dimensional ZrS_2 FET with both two-terminal and four-terminal configurations. The main aim is to characterize intrinsic optical properties of this less known compound for various electro-optic devices as a single component or in heterostructure, which is one of the current focuses of 2D research. We observed a significant improvement in photo conductivity with the four-terminal configuration, just by restricting the role of the contact resistance. The measured photoresponsivity (R) and external quantum efficiency (EQE) with the four–terminal configuration was enhanced by 1200% compared to that with the two-terminal measurements for the same device. These results are in good agreement with those for WSe_2 phototransistors in our recent study [31], in which we observed a 370% and a 461% higher photoresponsivity and EQE, respectively, with the four-terminal configuration. Thus, we believe that intrinsic electrical and optical properties of TMDs are significantly higher than their previously reported values, which opens new possibilities for improved photo-transistors and related devices where contact resistance play a significant role in measuring transport properties of the materials.

2. Results and Discussion

Few layered ZrS_2 single crystals were grown by chemical vapor transport (CVT) technique using the procedure used to grow other TMDs such as WSe_2, $MoSe_2$, MoS_2, ReS_2 etc. [29,31]. Thin layers of ZrS_2 were mechanically exfoliated from bulk crystal using scotch tape technique and subsequently transferred on to a clean 270 nm thick SiO_2 film grown on a p-doped Si substrate. Single to few-layered ZrS_2 flakes were identified by optical and atomic force microscopy. These layered crystals were characterized by Raman spectroscopy to verify their composition and crystal quality. Figure 1 presents the Raman spectrum of the ZrS_2 layer using a laser source of wavelength λ= 532 nm for varying thicknesses of ZrS_2 flakes. Here, the strong signal at 330 cm^{-1} represents the characteristic out-of-plane mode (A_{1g}) of ZrS_2, which increases with the sample thickness from bilayer (2L) to nearly twenty atomic layers (20L). The weak E_g mode is at 247 cm^{-1}. These observed Raman modes are similar to the previously observed Raman data on few-layered ZrS_2 crystals [35,36,39]. Figure 1 (b)-(d) display the optical micrograph images of layered ZrS_2 crystals exfoliated on to the Si/SiO_2 substrate. Raman data was collected from the several exfoliated flakes to verify the crystal quality. Supplementary Figure S1 shows AFM height image with height trace of one of the exfoliated ZrS_2 thin flakes.

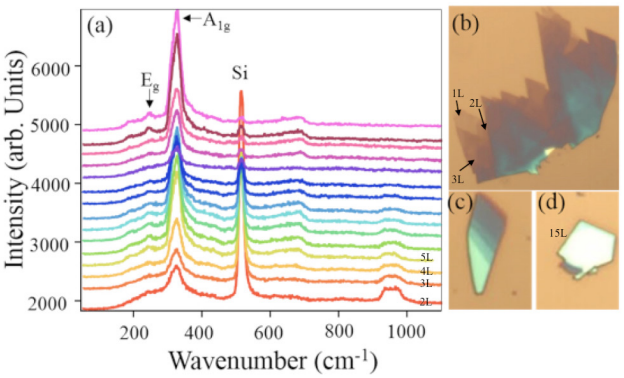

Figure 1. (a) Thickness dependent Raman spectrum of ZrS_2 crystals on Si/SiO_2 substrate. The Raman modes A_{1g} and E_g are labeled. (b)-(d) are the optical micrograph images of exfoliated ZrS_2 crystals showing single layer to few atomic layers of flakes

The field-effect transistor (FET) was fabricated on 285 nm thick p-doped Si/SiO_2 substrate by electron-beam lithography and electron beam evaporation technique. The devices were annealed at T = 300° C in forming gas followed by high vacuum annealing for 20 hours at 120° C. Figure 2(a) shows an optical micrograph image of a ZrS_2 FET device with four terminal contacts of Cr (5 nm)/Au (80 nm) with two voltage (V_1 and V_2) and two current leads (S and D) to measure the photoconductivity. To evaluate photon induced transport properties in the two-terminal configuration, the two voltage leads (S and D) were used to source voltage and measure the current of the device. The back-gate voltage (V_{bg}) was applied between the p-doped Si substrate and the source, and was varied to control the charge accumulation in the channel. Figure 2(b) illustrates the schematics of the FET and typical measurements obtained in the presence of a 532 nm laser under ambient conditions in a dark room environment. A dual channel Keithley Sourcemeter model 2612A was employed to apply the source-drain voltage (V_{ds}) (V_{ds} is applied between V_1 and V_2 in four-terminal configuration) and measure the source-drain current (I_{ds}), and the model 2635 was used to apply and control the gate voltage.

 DOI: https://doi.org/10.30564/ssid.v1i2.1526

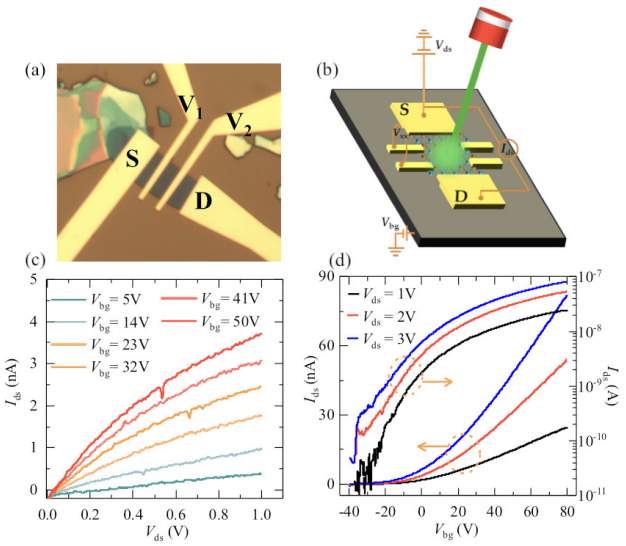

Figure 2. Optical micrograph image of ZrS_2 FET in multi-terminal contacts fabricated on the Si/SiO_2 substrate using Cr/Au (5/80 nm thick) metals. The thickness of the flake is 8-10 nm. (b) Schematic of the device and measurement scheme. (c) I_{ds} vs V_{ds} at several applied constant V_{bg} and (d) I_{ds} vs V_{bg} at constant V_{ds} = 1, V, 2V and 3V in the linear and logarithmic scale.

Figure 2(c) shows the source-drain current (I_{ds}) measured as a function of the source-drain voltage (V_{ds}) in the four-terminal configuration at several applied gate voltages (V_{bg}) from 5 V to 50 V. At lower V_{bg} values, 5 V and 14 V, the I_{ds} - V_{ds} plot shows a near linear behavior. This can be ascribed to the thermionic emission of carriers between metal contacts and ZrS_2 layer above the Schottky barrier at room temperature. However, for higher applied gate voltages (V_{bg}), the source-drain current (I_{ds}) starts displaying a non-linear variation with increasing source-drain voltage (V_{ds}). This nonlinear behavior can be attributed to non-ohmic contacts due to high Schottky barrier height between metal contacts and the few-layered ZrS_2 semiconducting channel. Figure 2(d) presents the measured I_{ds} as a function of applied gate voltage V_{bg} for constant source-drain voltages V_{ds} from 1 V to 3 V. The plot on the left current-axis displays the linear variation of I_{ds} with respect to V_{bg}. The I_{ds} with positive applied gate voltages (V_{bg}) affirms that the ZrS_2 sample is electron-doped or n-type FET. The plot using the right current-axis, shows the same variation of source-drain current (I_{ds}) in the semi-logarithmic scale as a function of V_{bg}. The observed ON to OFF current ratio of the few-layered ZrS_2 FET is 10^4. This current is much smaller than that showed by other TMDs such as MoS_2, WSe_2 reported in the literature but agrees with the results by Zhu et al. [38] on ZrS_2 FETs. Considering the linear region (V_{bg} > 50 V) of the I_{ds} vs V_{bg} plot, the four-terminal field-effect mobility of the FET can be calculated by the following equation [4,31].

$$\mu = \frac{l_v}{WC_i}\frac{1}{C_i}\frac{d(I_{ds}-I_o)/V_{ds}}{dV_{bg}} \quad (1)$$

Where, l_v is the length of the channel between voltage leads V_1 and V_2, V_{ds} (=V_{12}) is the voltage between V_1 and V_2, and I_o is the off current, W is the channel width. Ratio l_v/W for our device in 0.6. C_i is the gate capacitance per unit area, given by $C_i = \varepsilon\varepsilon_o/d$ = 11.7 x 10^{-9} F/cm^2. Where, ε and ε_o are the dielectric constant of SiO_2 and the permitivity of free space, respectively, and d is the thickness of the dielectric material, i.e. 285 nm for the SiO_2 layer used in our experiment. The four-terminal electron-mobility of this device calculated from equation (1) is 0.5-1 cm^2/Vs at room temperature. Similar mobilities of ZrS_2 FETs were reported previously on Si/SiO_2 substrate [36] or even when FET is fabricated on the h-BN substrate [37]. This value is much larger than the reported mobility by Shimazu et al. [39] measured on a 28 nm thick flake. In contrast, the four terminal mobilities of WSe_2 and MoS_2 are 145 cm^2/Vs [31] and 306 cm^2/Vs [4], respectively. This shows that ZrS_2 is too resistive; hence any attempt to find the two-terminal mobilities is highly affected by the contact resistance. In our previous studies on MoS_2 based FETs, we observed a similar pattern, i.e. the four-terminal mobility is significantly larger than the two-terminal mobility [4]. Mobility on ZrS_2 FET can be improved further by using suitable metal contacts or 2D metallic contacts like graphene and substrate where density of charge trap is lower than the rough Si/SiO_2 substrate. The low mobility could be attributed to defects and impurities in the crystals from CVT technique where transport agents were used for the synthesis.

We conducted both two-terminal and four-terminal photoconductivity measurements using a home-made microscope and data acquisition system equipped with a 532 nm monochromatic laser in darkroom environment. These values were compared with standard two-terminal photoconductivity measurements to evaluate the near intrinsic photoresponse of ZrS_2. More details of the experimental setup and the technique are explained in our previous study, performed to evaluate intrinsic photoresponse of WSe_2 [31]. Since the laser spot was larger than the sample size, the power illuminated on the sample P_{opt} can be estimated by,

$$P_{opt} = \frac{P}{\pi r^2}A \quad (2)$$

Where r, P and A are the radius of the laser spot, the power of the laser and the area of the sample, respectively. The radius of the laser spot (r) was measured using a lithographically patterned marker on the substrate. The dark current, I_{dark} was measured by varying the source-

DOI: https://doi.org/10.30564/ssid.v1i2.1526

drain voltage V_{ds} from 50 mV to 650 mV, in the absence of any laser illumination on the sample, i.e. $I_{dark} = I_{ds}$ for P = 0 W. The back-gate voltage (V_{bg}) was kept at -40 V to ensure that the device is in the OFF state. Next, I_{ds} was recorded as a function of P_{opt} by sweeping the laser power (P) from 10 nW to 50 μW using the attenuator. The back-gate voltage (V_{bg}) was fixed at -40 V and the source-drain voltage (V_{ds}) was varied from 50 mV to 650 mV for each set of measurements. The photo-induced current (I_{ph}) was calculated by subtracting the dark current from I_{ds} obtained by illuminating with light, i.e. $I_{ph} = I_{light} - I_{dark}$, measured at the same source-drain voltage (V_{ds}). I_{ph} shows a sudden rise and then a gradual increase with P_{opt} in both two and four-terminal configurations (See supporting information Figure S2). Figure-3 (a) and (b) show the photoresponsivity (R) of the device, $R = I_{ph}/P_{opt}$, as a function of optical power (P_{opt}) illuminated on the sample, for both two-terminal and four-terminal configurations. In the logarithmic scale, R decreases almost linearly as a function of increasing optical power, indicating that trap states in ZrS_2 layer or at the interface between ZrS_2 and SiO_2 play a dominant role. This indicates that ZrS_2 based FETs are suitable for high sensitive optical detection with low optical power as the trap states can significantly alter the sensitivity and efficiency of photo detectors. In addition, both the photocurrent and the photoresponsivity gradually increase with the source-drain voltage (V_{ds}). For the two-terminal configuration, the responsivity increases from 0.03 A/W at 50 mV to 0.5 A/W at 650 mV, when the optical power on the sample (P_{opt}) is approximately 90 nW. However, in the four-terminal configuration, the responsivity rises from 0.14 A/W at 50 mV to 6 A/W at 650 mV for the same (P_{opt}). Thus, the responsivity values extracted from the four-terminal measurements are significantly larger than the values extracted from two-terminal measurements. This increase in responsivity in four-terminal measurements is due to the elimination of contact resistance associated with the metal and semiconductor junction. The highest responsivity, R for two-terminal measurements, 0.5 A/W at V_{ds} = 650 mV and V_{bg} = -40 V, jumps to 6 A/W in the four-terminal measurements under the same V_{ds} and V_{bg}, which is nearly a 1200% enhancement. Our measured R value is much higher than the reported value for the same material by Wang et al. [36]. These values of R are also two orders of magnitude higher than the reported results by Mattinen et al., where they used Atomic Layer Deposition (ALD) method to synthesize large scale ZrS_2 crystals [40]. By fitting the responsivity as a function of optical power on the sample to the power law $R \propto P^{-\gamma}$, when V_{ds} = 650 mV, we obtained the γ = 0.84 and γ = 0.87 for the two-terminal and four-terminal configurations, respectively.

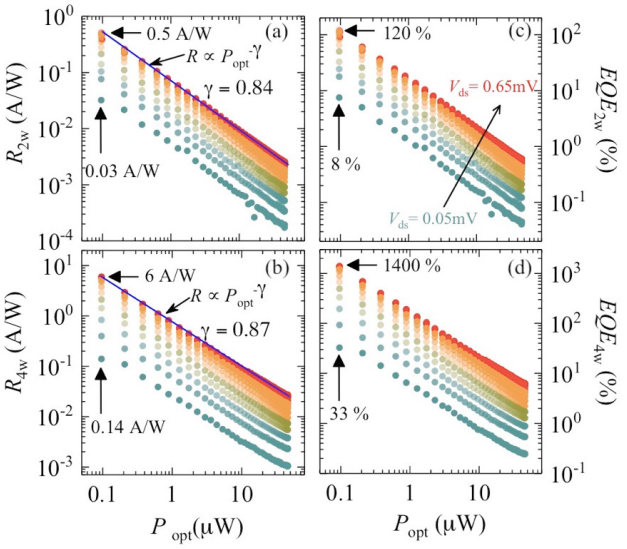

Figure 3. (a) and (b) display the photoresponsivity measured in two- and four-terminal configurations respectively as a function of incident optical power. (c) and (d) are the estimated external quantum efficiencies (EQE) for two- and four-terminal measurements for few layered ZrS_2 phototransistor. Blue solid lines in (a) and (b) are the least square fit to the experimental data

Next, we estimate the external quantum efficiency (EQE), which is defined as the number of electron-hole pairs generated by the number of photons illuminated on the phototransistor, using the following expression [10,31].

$$EQE = \frac{I_{ph}}{P_{opt}} \frac{hc}{\lambda q} = R \times \frac{hc}{\lambda q} \tag{3}$$

Where, P_{opt} is the optical power incident on the sample, h is the plank constant, c is the speed of light, λ is the wavelength of the laser source, and q is the electron charge. As shown in Figure 3 (c) and (d), the EQE follow a similar variation as R as a function of optical power (EQE $\propto R^{-\alpha}$). In the logarithmic scale, EQE decreases linearly with increasing P_{opt} at constant source-drain and back-gate voltages in the FET's OFF state, and EQE increases with the source-drain voltage for a given optical power on the sample. EQE increases from 8% to 120% when the source-drain voltage is increased from 50 mV to 650 mV in two-terminal measurements, however, it jumps from 33% to 1400% for the same source-drain voltage interval in the four-terminal configuration. This very high quantum efficiency of 1400% in four-terminal measurements compared to that estimated through two-terminal measurements, 120%, signifies that the four-terminal configuration produces a considerably higher EQE. This is nearly 1200% increase compared to the much adopted two-terminal configuration. In one of our previous studies to

 DOI: https://doi.org/10.30564/ssid.v1i2.1526

determine the photoresponsivity of WSe_2, we made a similar observation, where the EQE increased by 344% when it was estimated using a four-terminal configuration [31]. The linear decrease of EQE with increasing incident optical power has been observed for other 2D crystals [10,31] and believed to be a result of electron-hole recombination, which may have been stimulated by the radiation. However, the observed high EQE values in this study indicate that the recombination process is either hindered or enhanced by the generation of electron- hole pairs caused by the large surface to volume ratio of our few-layered ZrS_2 device. EQE values exceeding 100% suggests that one photon may have generated multiple electron-hole pairs, however the excitation frequency remains too low for this to occur. Studies performed by Li et. al. [41] and Ulanganathan et. al. [42] claim that high EQE and photoresponsivity are due to localized trapped states that slows the recombination process. They argue that one type of photo generated carriers is trapped in localized states, which expands the lifespan of the other carriers to circulate multiple times through the channel and source meters before the recombination. This process enhances the effective gain of the device as one photon seems to have created a substantially large photo-induced current due to slow a recombination process. This process yields EQE values exceeding 100%.

This study was performed for a single wavelength (λ=532 nm) as we focused on finding the dependence of photoresponsivity and photoinduced current on incident optical power in a multi-terminal configuration. The dark current was primarily due to thermally excited minority charge carriers. When the device is illuminated, the total current comes from thermally excited minority charge carriers (dark current), photogenerated current by electron-hole pairs, and the current induced by the photo thermoelectric effect (PTE) at the metal-semiconductor interface [43], as the whole device is exposed to the laser radiation, i.e. both the Cr/Au metal contacts and ZrS_2 semiconducting channel. Under laser illumination, the metal contacts become warmer than the semiconductor and their difference in Seebeck coefficients induces a net current flow across the metal-semiconductor interface, from the metal (hot) to semiconductor (cold) [43]. Since the size of the laser spot (700-800 μm^2) is much larger that the area of the device including metal contacts (100 μm^2), the net current flow across the channel due to PTE should be zero, as the currents from the two metal contacts to the semiconductor flow on opposite directions and cancels out. This leaves the dark current and the photogenerated current as contributing factors when the device is under illumination.

The dependence of R and EQE in the four-terminal configuration with the source-drain voltage (V_{ds}) in the logarithmic scale is shown in Figure 4, based on extracted data from Figure 3 (c) and (d), for selected incident optical powers. Upon fitting with the power law ($R \propto V^{-\alpha}$), we found that the dependence of R with V_{ds} is slightly non-linear with exponent α=1.6. The highest value estimated for R is 6 A/W at V_{ds} = 650 mV and P_{opt} = μW that significantly decreases as we increase the optical power. However, previous studies have reported very high responsivities for WSe_2 phototransistors under ultra-low incident optical power and higher bias voltages [28]. This mismatch might have come from the low absorption of ZrS_2 at 532 nm compared to that of WSe_2. ZrS_2 shows high absorption in the range of 300 nm to 400 nm in heterostructure geometry with h-BN or graphene compared to 532 nm in WSe_2 [44]. The responsivity also largely depends upon the incident optical power, applied drain-source and gate voltages used. As an example, a high R of 880 A/W was reported for monolayer MoS_2 based FETs under a very low incident optical power of 150 pW (V_{ds} = 8 V and V_{bg} = -70 V), which sharply dropped to 4 A/W as the incident optical power increased to 250 nW [20]. In comparison, the R value estimated in our study for ZrS_2 FET at 250 nW (0.25 μW) and V_{ds} = 650 mV (0.65 V) is approximately 2 A/W (Fig- ure 3 b), which can be extrapolated to approximately 110 A/W at V_{ds} = 8 V (Figure 4 a). This is in good agreement with our previous study on few-layered WSe_2, which shows a very high R value when it was measured with the four-terminal configuration (R = 85 A/W at P_{opt} = 248 nW and V_{ds} = 1 V) [31]. This illustrates that the four-terminal configuration-based measurements have resulted in a much higher R and EQE values than those of previously reported on ZrS_2 phototransistor.

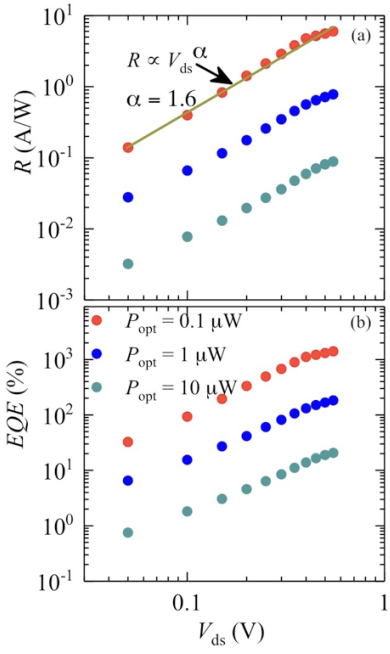

Figure 4. (a) Responsivity and (b) EQE as a function of V_{ds} extracted at constant illuminated optical power. Red line represents the fitting of R in power law to extract the exponent α

DOI: https://doi.org/10.30564/ssid.v1i2.1526

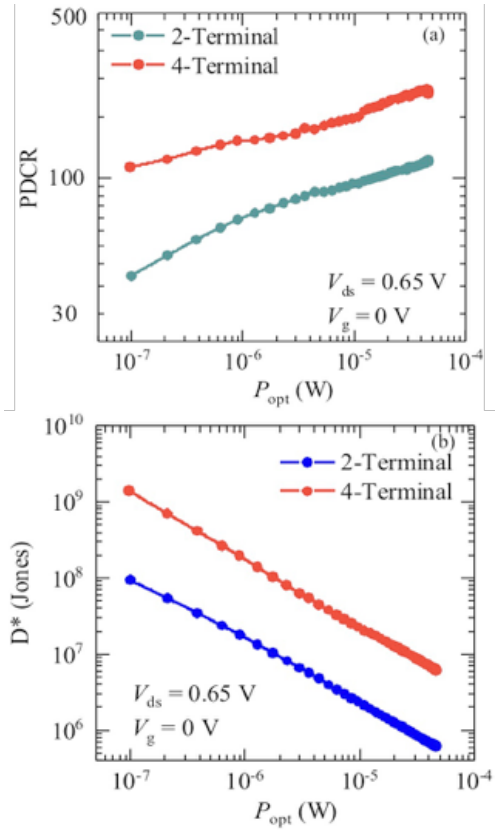

Figure 5. (a) PDCR and (b) Detectivity of few layered ZrS2 phototransistor as a function of illuminated optical power

We further explored the photo dark current ratio (PDCR) and detectivity (D) of our ZrS_2 based photo-transistor as presented in Figure 5, which demonstrates the photodetection application and the figure of merit to use for the performance of photodetector of ZrS_2 based phototransistor. PDCR is estimated by measuring the ratio of photocurrent and dark current (PDCR = $(I_{light} - I_{dark})/I_{dark} = I_{ph} / I_{dark}$, where I_{light} is the current measured with light illuminated and I_{dark} is the dark current with no light illumination. Figure 5 (a) shows the PDCR values of few layered ZrS_2 measured in two and four-terminal configurations as a function of increasing optical power. The PDCR values measured in 4-terminal method ranges between 100 at 0.1 μW and 275 at 0.4 mW optical power under applied V_{ds} = 0.65 V, which are much higher than some of the reported photodetectors currently in use such as AlN, GaN, SiC, Ga_2O_3 etc. [45-48] and similar to the MoS_2 photodetector reported earlier [26]. The specific detectivity is extracted from the relation given by $D^* = R\sqrt{A} / \sqrt{2qI_{dark}}$, where R is the photoresponsivity, A is the area of the detector, q is the unit of charge, and I_{dark} is the dark current. As shown in Figure 5 b, D^* varies linearly with optical power from 10^7 Jones at 1 mW power to 10^9 Jones at 0.1 μW incident optical power in the OFF state of the transistor (V_{bg} = 0 V) and small V_{ds} = 0.065 V. Similar detectivities were also reported on few layered MoS_2 [26]. Higher value of the detectivity can be obtained in the ON state of the transistor and by applying higher V_{ds} [30].

3. Conclusion

We report the intrinsic photo transport properties of few layered ZrS_2 phototransistors measured with multi- terminal configuration. We studied the dependence of photocurrent, photoresponsivity and the external quantum efficiency as a function of incident optical power and bias voltage when the FET is in the OFF state at a fixed back-gate voltage. The estimated photoresponsiv ity R and EQE values show that four-terminal measurements result extremely high values, at least one order of magnitude higher than that with two-terminal configurations. This clearly indicates that the optical properties of FETs based on few-layered TMDs can be significantly enhanced by minimizing the contact resistance. Here, the ZrS_2 FET with approximately 10 atomic layers of ZrS_2 shows an impressive R and EQE values through four-terminal measurements representing an improvement of 1200%, over the values estimated through traditional two-terminal configuration. Furthermore, few-layered ZrS_2 shows an excellent photo sensitivity factor (PDCR) that is up to 275 at low applied bias and zero gate voltage when measured in four-terminal configuration. Few-layered ZrS_2 also shows high detectivity at low incident optical power. This signifies that a four-terminal configuration is more suitable when investigating intrinsic optoelectronic properties of TMD based FETs, particularly 2D materials where contact resistance plays a crucial role to determinate of incident the intrinsic transport properties, which can be ultimately utilized for the fabrications of devices that require high yields and high sensitivities. We believe that measuring the intrinsic optoelectronic properties of 2D materials, TMDs would make them promising candidates for a wide range of future applications. The electrical and optical properties of ZrS_2 reported here will guide to fabricate heterostructure devices based 2D TMDS where ZrS_2 can provide the high yields and sensitivities required for optical applications.

Acknowledgments

N. R. P. acknowledged NSF-PREM through NSF-DMR-1826886, HBCU-UP Excellence in research NSF-DMR-1900692. A portion of this work was performed at the National High Magnetic Field Laboratory, which is supported by the National Science Foundation Cooperative Agreement No. DMR-1644779 and the State of Flor-

 DOI: https://doi.org/10.30564/ssid.v1i2.1526

ida. This work was performed, in part, at the Center for Nanoscale Materials, a U.S. Department of Energy Office of Science User Facility, and supported by the U.S. Department of Energy, Office of Science, under Contract No. DE-AC02-06CH11357.

Supporting Information

The supplementary materials contain the Figure S1, which is the variation of photocurrent as a function of incident optical power under different bias voltages for both two-terminal and four- terminal configurations.

Supplementary Materials

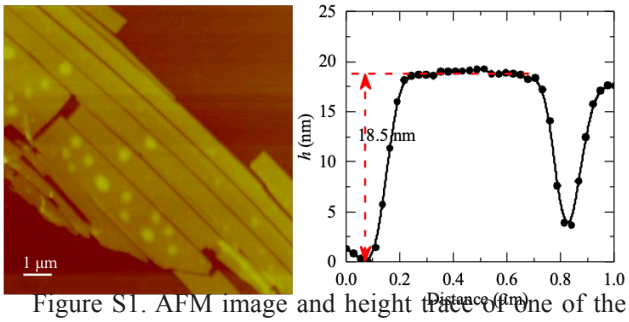

Figure S1. AFM image and height trace of one of the exfoliated flakes of ZrS_2 on to Si/SiO_2 substrate

Note: AFM height measurements were performed on several exfoliated crystals of ZrS_2 on Si/SiO_2 substrate using Veeco Dimension 3100 AFM setup. The flakes used for optical measurements are from 8 nm to 15 nm thick.

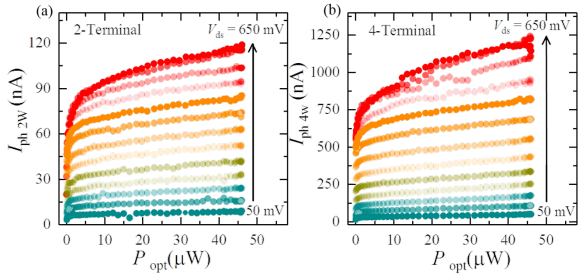

Figure S2. Photocurrent vs incident optical power

Note: The photocurrent as a function of incident optical power under several bias voltages for (a) two-terminal configuration (b) four-terminal configuration (I_{ph2W} and I_{ph4W} denote the photocurrent with two and four-terminal configurations, respectively). The four-terminal photocurrent is significantly larger (>1000 %) than the two-terminal current. Under both configurations, the photocurrent increases with the bias voltage.

References

[1] H. Wang, L. Yu, Y. H. Lee, Y. Shi, A. Hsu, M. L. Chin, L.J. Li, M. Dubey, J. Kong, T. Palacios. Integrated circuits based on bilayer MoS2 transistors, Nano letters, 2012, 12: 4674.

[2] B. Radisavljevic, A. Radenovic, J. Brivio, V. Giacometti, A. Kis. Single-layer MoS2 transistors, Nature nanotechnology, 2011, 6: 147.

[3] N. R. Pradhan, D. Rhodes, S. Feng, Y. Xin, S. Memaran, B.-H. Moon, H. Terrones, M. Terrones, and L. Balicas, Field-effect transistors based on few-layered α-MoTe2, ACS nano, 2014, 8: 5911.

[4] N. Pradhan, D. Rhodes, Q. Zhang, S. Talapatra, M. Terrones, P. Ajayan, L. Balicas. Intrinsic carrier mobility of multi-layered mos2 field-effect transistors on SiO2, Applied Physics Letters, 2013, 102: 123105.

[5] N. R. Pradhan, D. Rhodes, Y. Xin, S. Memaran, L. Bhaskaran, M. Siddiq, S. Hill, P. M. Ajayan, L. Balicas. Ambipolar molybdenum diselenide field-effect transistors: field-effect and hall mobilities, Acs Nano, 2014, 8: 7923.

[6] N. R. Pradhan, J. Ludwig, Z. Lu, D. Rhodes, M. M. Bishop, K. Thirunavukkuarasu, S. A. McGill, D. Smirnov, L. Balicas. High photoresponsivity and short photoresponse times in few-layered WSe2 transistors, ACS applied materials & interfaces, 2015, 7: 12080.

[7] S. Memaran, N. R. Pradhan, Z. Lu, D. Rhodes, J. Lud- wig, Q. Zhou, O. Ogunsolu, P. M. Ajayan, D. Smirnov, A. Fernandez-Dom´ınguez, et al.. Pronounced photovoltaic response from multilayered transition-metal dichalcogenides pn-junctions, Nano letters, 2015, 15: 7532.

[8] N. R. Pradhan, Z. Lu, D. Rhodes, D. Smirnov E. Manousakis, L. Balicas. An optoelectronic switch based on intrinsic dual schottky diodes in ambipolar MoSe2 field-effect transistors, Advanced Electronic Materials, 2015, 1: 1500215.

[9] N. R. Pradhan, C. Garcia, B. Isenberg, D. Rhodes, S. Feng, S. Memaran, Y. Xin, A. McCreary, A. R. H. Walker, A. Raeliarijaona, et al.. Phase modulators based on high mobility ambipolar rese 2 field-effect transistors, Scientific reports, 2018, 8: 12745.

[10] C. Garcia, N. Pradhan, D. Rhodes, L. Balicas. S. McGill. Photogating and high gain in res2 field-effect transistors, Journal of Applied Physics, 2018, 124: 204306.

[11] G. Fiori, F. Bonaccorso, G. Iannaccone, T. Palacios, D. Neumaier, A. Seabaugh, S. K. Banerjee, L. Colombo. Electronics based on two-dimensional materials, Nature nanotechnology, 2014, 9: 768.

[12] Q. H. Wang, K. Kalantar-Zadeh, A. Kis, J. N. Coleman, M. S. Strano. Electronics and optoelectronics of two-dimensional transition metal dichalcogenides, Nature nanotechnology, 2012, 7: 699.

[13] W. Zhang, Z. Huang, W. Zhang, Y. Li. Two-dimensional semiconductors with possible high room temperature mobility, Nano Research, 2014, 7: 1731.

[14] H. Guo, N. Lu, L. Wang, X. Wu, X. C. Zeng, Tuning

DOI: https://doi.org/10.30564/ssid.v1i2.1526

electronic and magnetic properties of early transition-metal dichalcogenides via tensile strain, The Journal of Physical Chemistry C, 2014, 118: 7242.

[15] Y. Li, J. Kang, J. Li. Indirect-to-direct band gap transition of the ZrS2 monolayer by strain: first- principles calculations, Rsc Advances, 2014, 4, 7396.

[16] A. Kumar, H. He, R. Pandey, P. Ahluwalia, K. Tankeshwar, Semiconductor-to-metal phase transition in monolayer ZrS2: Gga+ u study, in AIP Conference Proceedings (AIP Publishing, 2015, 1665: 090016.

[17] H. J. Conley, B. Wang, J. I. Ziegler, R. F. Haglund Jr, S. T. Pantelides, K. I. Bolotin. Bandgap engineering of strained monolayer and bilayer MoS2, Nano letters, 2013, 13: 3626.

[18] T. Cheiwchanchamnangij, W. R. Lambrecht, Quasi-particle band structure calculation of monolayer, bilayer, and bulk MoS2, Physical Review B, 2012, 85: 205302.

[19] K. F. Mak, C. Lee, J. Hone, J. Shan, T. F. Heinz, Atomically thin MoS2: a new direct gap semiconductor, Physical review letters, 2010, 105: 136805.

[20] O. Lopez-Sanchez, D. Lembke, M. Kayci, A. Raden-ovic, A. Kis. Ultrasensitive photodetectors based on monolayer MoS2, Nature nanotechnology, 2013, 8: 497.

[21] Z. Yin, H. Li, H. Li, L. Jiang, Y. Shi, Y. Sun, G. Lu, Q. Zhang, X. Chen, H. Zhang. Single-layer MoS2 phototransistors, ACS nano, 2011, 6: 74.

[22] D. Kufer, G. Konstantatos. Highly sensitive, encapsulated MoS2 photodetector with gate controllable gain and speed, Nano letters, 2015, 15: 7307.

[23] J. Pak, J. Jang, K. Cho, T.-Y. Kim, J.-K. Kim, Y. Song, W.-K. Hong, M. Min, H. Lee, T. Lee. Enhancement of photodetection characteristics of MoS2 field effect transistors using surface treatment with copper phthalocyanine, Nanoscale, 2015, 7: 18780.

[24] G. Wu, X. Wang, Y. Chen, Z. Wang, H. Shen, T. Lin, W. Hu, J. Wang, S. Zhang, X. Meng, et al.. Ultrahigh photoresponsivity MoS2 photodetector with tunable photocurrent generation mechanism, Nanotechnology, 2018, 29: 485204.

[25] W. Choi, M. Y. Cho, A. Konar, J. H. Lee, G.-B. Cha, S. C. Hong, S. Kim, J. Kim, D. Jena, J. Joo, et al.. High-detectivity multilayer MoS2 phototransistors with spectral response from ultraviolet to infrared, Advanced materials, 2012, 24: 5832.

[26] D.-S. Tsai, K.-K. Liu, D.-H. Lien, M.-L. Tsai, C.-F. Kang, C.-A. Lin, L.-J. Li, J.-H. He. Few-layer MoS2 with high broadband photogain and fast optical switching for use in harsh environments, Acs Nano, 2013, 7: 3905.

[27] H. S. Lee, S.-W. Min, Y.-G. Chang, M. K. Park, T. Nam, H. Kim, J. H. Kim, S. Ryu, S. Im. Mos2 nanosheet phototransistors with thickness-modulated optical energy gap, Nano letters, 2012, 12: 3695

[28] A. Abderrahmane, P. Ko, T. Thu, S. Ishizawa, T. Takamura, and A. Sandhu, High photosensitivity few-layered MoSe2 back-gated field-effect phototransistors, Nanotechnology 25, 365202 (2014).

[29] N. Pradhan, D. Rhodes, S. Memaran, J. Poumirol, D. Smirnov, S. Talapatra, S. Feng, N. Perea-Lopez, A. Elias, M. Terrones, et al.. Hall and field-effect mobilities in few layered *p*-WSe2 field-effect transistors, Scientific reports, 2015, 5: 8979.

[30] W. Zhang, M.-H. Chiu, C.-H. Chen, W. Chen, L.-J. Li, A. T. S. Wee. Role of metal contacts in high-performance phototransistors based on wse2 monolayers, ACS nano, 2014, 8: 8653.

[31] N. R. Pradhan, C. Garcia, J. Holleman, D. Rhodes, C. Parker, S. Talapatra, M. Terrones, L. Balicas, S. A. McGill, Photoconductivity of few-layered *p*-WSe2 phototransistors via multi-terminal measurements, 2D Materials, 2016, 3: 041004.

[32] N. Huo, S. Yang, Z. Wei, S.-S. Li, J.-B. Xia, J. Li, Photoresponsive and gas sensing field-effect transistors based on multilayer WS2 nanoflakes, Scientific reports, 2014, 4: 5209.

[33] N. R. Pradhan, A. McCreary, D. Rhodes, Z. Lu, S. Feng, E. Manousakis, D. Smirnov, R. Namburu, M. Dubey, A. R. Hight Walker, et al.. Metal to insulator quantum-phase transition in few-layered ReS2, Nano letters, 2015, 15: 8377.

[34] Y. Wen, Y. Zhu, S. Zhang. Low temperature synthesis of ZrS2 nanoflakes and their catalytic activity, RSC Advances, 2015, 5: 66082.

[35] S. Manas-Valero, V.Garcıa-Lopez, A.Cantarero, M. Galbiati. Raman spectra of ZrS2 and ZrSe2 from bulk to atomically thin layers, Applied sciences, 2016, 6: 264.

[36] X. Wang, L. Huang, X.-W. Jiang, Y. Li, Z. Wei, J. Li. Large scale ZrS2 atomically thin layers, Journal of Materials Chemistry C, 2016, 4: 3143.

[37] M. Zhang, Y. Zhu, X. Wang, Q. Feng, S. Qiao, W. Wen, Y. Chen, M. Cui, J. Zhang, C. Cai, et al.. Controlled synthesis of ZrS2 monolayer and few layers on hexagonal boron nitride, Journal of the American Chemical Society, 2015, 137: 7051.

[38] Y. Zhu, X. Wang, M. Zhang, C. Cai, L. Xie. Thickness and temperature dependent electrical properties of ZrS2 thin films directly grown on hexagonal boron nitride, Nano Research, 2016, 9: 2931.

[39] Y. Shimazu, Y. Fujisawa, K. Arai, T. Iwabuchi, and K. Suzuki, Synthesis and characterization of zirconium disulfide single crystals and thin-film transis-

 DOI: https://doi.org/10.30564/ssid.v1i2.1526

tors based on multilayer zirconium disulfide flakes, ChemNanoMat, 2018, 4: 1078.

[40] M. Mattinen, G. Popov, M. Vehkamaki, P. J. King, K. Mizohata, P. Jalkanen, J. Raisanen, M. Leskela, M. Ritala. Atomic layer deposition of emerging 2d semiconductors, HfS2 and ZrS2, for optoelectronics, Chemistry of Materials,2019, 31: 5713.

[41] X. Li, J. Carey, J. Sickler, M. Pralle, C. Palsule, C. Vineis, Silicon photodiodes with high photoconductive gain at room temperature, Optics Express, 2012, 20: 5518.

[42] R. K. Ulaganathan, Y. Y. Lu, C. J. Kuo, S. R. Tamalampudi, R. Sankar, K. M. Boopathi, A. Anand, K. Yadav, R. J. Mathew, C.-R. Liu, et al.. High photosensitivity and broad spectral response of multi-layered germanium sulfide transistors, Nanoscale, 2016, 8: 2284.

[43] N. Perea-Lopez, Z. Lin, N. R. Pradhan, A. Iniguez Rabago, A. L. Elıas, A. McCreary, J. Lou, P. M. Ajayan, H. Terrones, L. Balicas, et al., CVD-grown monolayered MoS2 as an effective photosensor operating at low- voltage, 2D Materials 1, 011004, 2014.

[44] X. Zhang, Z. Meng, D. Rao, Y. Wang, Q. Shi, Y. Liu, H. Wu, K. Deng, H. Liu, R. Lu. Efficient band structure tuning, charge separation, visible-light response in ZrS2-based Van der Waals heterostructures, Energy & Environmental Science, 2016, 9: 841.

[45] H. So, D. G. Senesky, ZnO nanorod arrays and direct wire bonding on GaN surfaces for rapid fabrication of antireflective, high-temperature ultraviolet sensors, Applied Surface Science, 2016, 387: 280.

[46] D. S. Tsai, W. C. Lien, D. H. Lien, K. M. Chen, M. L. Tsai, D. G. Senesky, Y. C. Yu, A. P. Pisano, J. H. He, Solar-blind photodetectors for harsh electronics, Scientific reports, 2013, 3: 2628.

[47] C. Lien, D. S. Tsai, S. H. Chiu, D. G. Senesky, R. Maboudian, A. P. Pisano, and J. H. He, Low temperature, ion beam-assisted sic thin films with antireflective ZnO nanorod arrays for high temperature photodetection, IEEE Electron Device Letters, 2011, 32, 1564.

[48] T. C. Wei, D. S. Tsai, P. Ravadgar, J. J. Ke, M. L. Tsai, D. H. Lien, C. Y. Huang, R. H. Horng, J. H. He. See-through Ga2O3 solar-blind photodetectors for use in harsh environments, IEEE Journal of Selected Topics in Quantum Electronics, 2014, 20: 112.

DOI: https://doi.org/10.30564/ssid.v1i2.1526